

NUMERICAL REQUIREMENTS FOR THE USE OF A THCM MATERIAL MODEL TO THE PREDICTION OF EARLY AGE CRACKING RISK OF MASSIVE REINFORCED CONCRETE STRUCTURES

P. CHHUN^{*}, L. LACARRIERE[†] AND A. SELLIER^{††}

Université de Toulouse; UPS, INSA; LMDC

135, avenue de Rangueil, 31 077 Toulouse Cedex 04, France

e-mail: ch_ponleu@yahoo.com^{*}

laurie.lacARRIERE@insa-toulouse.fr[†]

sellier@insa-toulouse.fr^{††}

Key words: Early age, Cracking, Shrinkage, Concreting sequence, Distributed reinforcement, Reinforced concrete

Abstract: The work presented here was carried out in the framework of the French MACENA project (ANR-PIA) dealing with the control confinement of nuclear containment. In this project, one of the aspects studied was the study of the risk of early cracking of the lower parts of the containment (basement and gusset). Indeed, these parts are sufficiently massive parts to risk developing short-term cracking due to temperature changes within the restrained structure at an early age. This early age cracking has been identified at later ages as an important part of the causes of leakage of the structure and is thus of importance in the control of confinement. The work presented here focused in particular on the modelling of a containment vessel mock-up built by EDF (VeRCoRs). In this mock up, instrumentation and visual inspections of the gusset made it possible to characterize the evolution of temperatures, strains and cracking pattern in the first months after casting of these sensitive parts of the structure.

The early age behavior model developed at the LMDC in recent years [1]–[3] is used to reproduce the behavior of concrete. But the application to very large reinforced concrete structures required the development of specific digital tools that were complementary to the model of early behavior. The article therefore focus on presenting these adaptations of the material model to a structural application through three main aspects: the consideration of a casting phasing, the consideration of reinforcements by macro elements that allows avoiding an explicit mesh of reinforcements and finally the consideration of the variability of the material on the tensile strength of concrete. These developments are presented and applied to the modelling of the behavior of the basement and gusset of the VeRCoRs mock-up at early age. The experimental measurements enable to test and validate the numerical models for reproducing the most likely behavior of the structure.

1 INTRODUCTION

The work presented here was performed in the context of the project ANR-PIA MACENA. The study is part of the project dealing with the early age behavior of reinforced concrete under thermo-hydro-chemo-mechanical

(THCM) loads. One of the objectives of this study was to perform some numerical studies using models on a real experimental mock-up of a reactor, called VeRCoRs at early age.

In the international literature, several recent studies have focused on the finite element modelling of the early-age behavior of massive concrete structures. However, many of them are more concerned with validating a thermal model and propose a purely numerical analysis of mechanical aspects [4]–[6]. Only a few studies focused on early-age cracking and crack patterns are also compared [7]–[9] but as instrumentation of real case massive structures is difficult to perform, mechanical results at early age (strains) are not usually compared (only a few reference is available in the literature [2], [10]).

In this context, the French national project ANR-PIA MACENA proposes to study vessel mock-up VeRCoRs which was finely instrumented so that its behaviors (local temperature and strains) could be monitored from the beginning of the construction (**FIGURE 1**).



Figure 1: Nuclear reactor building VeRCoRs mock-up [12]

For this massive structure, concrete was cast in successive layers at a different time to limit the high rise of temperature, the segregation of aggregates in concrete and facilitate the concrete pouring. However, additional checks are also required for the analysis of staged construction because the strains in the young concrete layer are restrained by the previous concrete layers and tensile stresses arise and induce the early cracking if the stress becomes greater than the strength of the material.

Consequently, structural damage may occur before the main loading such as during LOCA, and the durability and serviceability of the construction may be significantly reduced. More importantly, when cracking problem is addressed, the estimation of current tensile strength which is linked to the heterogeneity of concrete according to the CEOS.fr conclusions [11], becomes crucial. Nowadays, numerical tools taking the scale effect, which is a characteristic of heterogeneous materials, into account are progressively enriched. One, among these methods, based on WL2 theory will be emphasized and used in this study.

The aim of this paper is to simulate the early-age cracking of this kind of massive structure and especially the effect of reinforcement and scale effect on the prediction of cracking pattern.

2 PRESENTATION OF NUCLEAR CONTAINMENT MOCK-UP VERCORS

In the framework of EDF's continuous effort on the safety and life extensions of nuclear power plants, an experimental mock-up of a reactor containment-building at 1/3 scale was built at Renardieres near Paris. The so-called VeRCoRs mock-up is a double wall containment ($H=30\text{m}$; $\varnothing=16\text{m}$). This mock-up was constructed in different stages such as pedestal foundation, basement, gusset, wall and dome. The evolution of temperature of this structure was recorded by thermocouples from the start of construction.

3 PRESENTATION OF THCM MODEL-LMDC

In this paper dedicated to the numerical results obtained in the framework of ANR-PIA MACENA, only three main aspects are presented here: the strategy for concreting sequence modelling, the consideration of reinforcements by macro elements and the consideration of the variability of the material on the tensile strength of concrete via the probabilistic scale effect. Details of the model equations and implementation can be found in the references in the following paragraphs.

The THCM model for early-age concrete is based on weak coupling between a hydration model [13] and a mechanical model adapted for hardening concrete [3], [14].

3.1 Strategy for concreting sequence modelling

The nuclear reactor building is constructed at different stages. Analysis of the temperature field due to hydration of concrete is a highly non-linear problem due to several reasons. The sequential casting is time-dependent and the filling sequences of the formwork are superimposed at different times. The thermal heat exchange between the concrete and the atmosphere is affected by the formwork, wind flow and external temperature. All these transient boundary conditions have to be taken into account in the finite element model. In this work, a multiphasic hydration model is used to simulate the thermo-hydro-chemical behavior of early-age concrete. This study is essential to assess the initial state of the structure before the loss-of-coolant accident (LOCA) because it provides the input data for the mechanical modelling.

Each stage of concrete may be modelled using different meshes by separate analyses. However, separate analyses cannot reproduce the most likely behavior of each element because the successive elements can effect on each other.

To avoid the separate analyses, a better strategy for modelling the sequential casting is introduced here. This method presents several advantages. First, it facilitates the mesh of structure. Each element of the whole structure can be meshed at the same time, but the model is activated once the concrete is cast. Moreover, it takes the behavior of computed concrete into account for next calculation of new concrete.

The method consists of meshing each element of structure and activating the hydration model only if the element is cast. The activation of the hydration model is made

introducing a delayed coefficient P_{sup} in the hydration affinity law.

The parameter P_{sup} is equal to zero when the time t is lower than the casting time $t_{casting}$ of the geometrical zone, and to 1 as soon as the time reach the casting date (Equation (1)).

$$P_{sup} = \begin{cases} 0 & \text{if } t < t_{casting} \\ 1 & \text{if } t \geq t_{casting} \end{cases} \quad (1)$$

3.2 Adaptation for reinforced concrete structure

Regarding the limits of the existing approaches (stress concentration, meshing difficulty, and capacity to be applied to either fine or coarse mesh, applicability for large-scale structure...), a new approach (Figure 2) is proposed in this contribution which is adapted to concrete model for an application of large-scale structures such as nuclear containment.

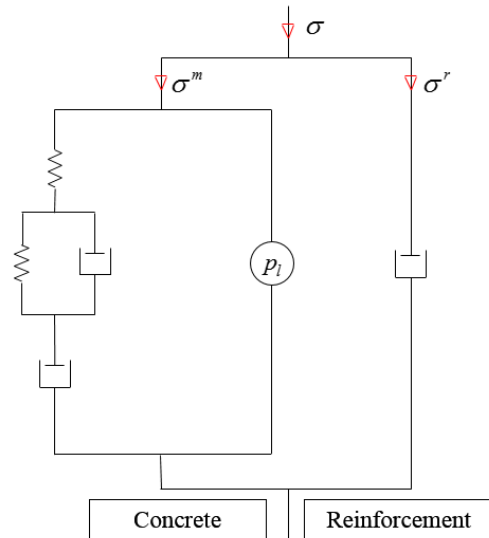


Figure 2: Idealized scheme for modelling reinforced concrete

The so-called “Distributed reinforcement” can be used in 3D FE domain using the ratio of steel cross-section inside the concrete in any direction without additional mesh of reinforcements.

In particular, it aims at providing the structural effect of reinforcements (without stress concentration) in nonlinear solid mechanic

problems involving various types of behavior laws for the reinforcement and matrix and solved by the finite element method.

This alternative approach is based on the principle of the homogenized behavior of the reinforced matrix. It is described via the combination of steel and concrete stresses which are modified upon their directions (\overline{V}^r , with $r \in [1, \dots, n^r]$ and n^r the distributed reinforcement number) and is written by Eq. (2).

$$\sigma_{ij} = (1 - \rho^r) \sigma_{ij}^m + \rho^r \sigma^r \quad (2)$$

With ρ^r is the cross-section ratio of the reinforcement oriented along the axe \overline{V}^r . σ_{ij}^m is the total stress in the matrix and σ_i^r is the axial stress in the reinforcement computed in each direction of reinforcement by equation (3). The behavior law of reinforcement is elastoplastic with a linear kinetic hardening and a relaxation law.

$$\sigma^r - \sigma_0^r = E^r (\varepsilon^r - \varepsilon^{r,pl} - \varepsilon^{r,m} - \varepsilon^{r,k}) \quad (3)$$

Where E^r the reinforcement Young modulus, ε^r the axial strain in the reinforcement, $\varepsilon^{r,pl}$ its plastic strain, $\varepsilon^{r,m}$ its permanent viscous strain and $\varepsilon^{r,k}$ its reversible viscous strain. σ_0^r is the possible pre-stress applied to the reinforcement as initial stress (not induced by the computed strain field).

The plastic criterion of reinforcement is uniaxial and it models a linear kinetic hardening:

$$f^r = |\sigma^r - H^r \varepsilon^{r,pl}| \leq f_y^r \quad (4)$$

In Eq. (4), H^r is the hardening modulus and f_y^r is the elastic limit for the reinforcements.

This modelling method of distributed reinforcement was tested and validated on a reinforced beam which was used firstly in a theoretical case study in the numerical

benchmark MECA, in 2003 [15], and by other authors [17]. This study can be found in [18].

3.3 PROBABILISTIC SCALE EFFECT

After receiving the data on mechanical properties from different partners in MACENA project, we can notice a remarkable dispersion of the values in Figure 7, especially at 28 days. The tensile strength is an important criteria to treat the cracking of concrete, but it's hardly to find its reliable value despite a large amount of samples because there is another impact of material heterogeneity which is unavoidable particularly for massive structure like reactor VERCORS. Fortunately, the random distribution of tensile strength leading to a probabilistic scale effect can be dealt with an alternative approach, called "Weakest Link Localization" [19] thank to the Weibull's concept. This approach is capable to assess directly the most likely tensile strength, which treats the first crack in a softening part of the loaded volume of structures, via the following law (Eq. (5)). The scale effect can be presented through the curve (Figure 8) that shows the diminution of tensile strength when the size of volume increases.

$$\frac{R_{t(M)}}{R_t^{ref}} = \left(\frac{V_{ref}}{V_{eq(M)}} \right)^{1/m} \quad (5)$$

In Eq. (5), $R_{t(M)}$ is a tensile strength at point M. R_t^{ref} is the average tensile strength measured on a specimen with the loaded volume V_{ref} . m is the Weibull exponent

depending on the coefficient of variation C^v of experimental results:

$$m \approx \frac{1}{10} \left(\frac{12}{C^v} - 2 \right) \quad (6)$$

And the equivalent loaded volume $V_{eq(M)}$ is defined as follows:

$$V_{eq(M)} = \frac{1}{\beta_{max}} \int_{\Omega} \beta \cdot \psi(M) d\Omega \quad (7)$$

With $\psi(M)$ the weighting function (8), β the loading index (9), Ω the structure, and $d\Omega$ a structure infinitesimal volume.

$$\psi(M) = \exp\left[-\frac{1}{2}\left(\frac{d(M)}{l_{cp}}\right)^2\right] \quad (8)$$

Where $d(M)$ the distance between point M and its nearby point, l_{cp} the characteristic length of probabilistic weighting function whose usual value is $0.5m$ for a concrete.

$$\beta = \left(\frac{\max(\sigma_t, 0)}{R_t^{ref}}\right)^m \quad (9)$$

With σ_t the principal tensile stress

4 APPLICATION TO THE LOWER PART OF VESSEL MOCK-UP VERCORS

The structure studied in this paper is a lower part of the internal containment (Figure 4). It contains pedestal, basement, gusset and interior wall.

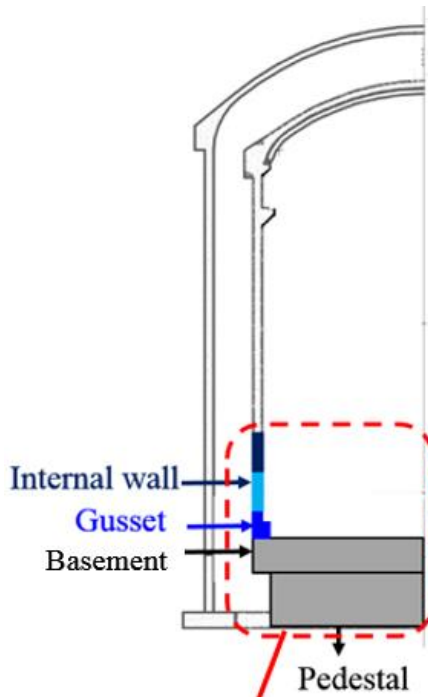


Figure 3: Axisymmetric section of structure VERCORS

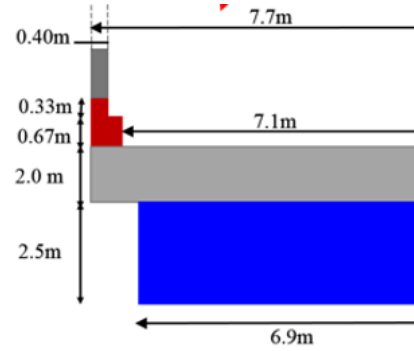


Figure 4: Detail of gusset and raft

4.1 Formulation of concrete for VeRCoRs and its environmental conditions

The concrete used in the structure was cast with a CEM I 52.5N cement. The formulation is given in Table 1.

It is necessary to consider in the model the environmental conditions of structure such as ambient temperature, wind flow and formwork properties in order to obtain the most likely evolution of temperature field in the structure. Concrete was cast, for massive structure, at different stages. The initial temperature of concrete for each stage is used in the model as the initial condition and the daily variation of external temperature was considered directly in the model through convective boundary condition. Details of this information can be found in [18].

Table 1: Formulation of VeRCoRs concrete

	Quantities (kg/m ³)
Cement CEM I 52.5N CE CP2 NF Gaurain	320
Sand 0/4 rec GSM LGP1	830
Gravel 4/11R GSM LGP1	445
Gravel 8/16R Balloy	550
Superplasticizer Techno 80	2.4
Effective water	167.2

4.2 Identification of model and material parameters

The three fitting parameters of the multiphasic hydration model (managing hydration, temperature, and water content evolution) were determined by an inverse analysis on an isothermal calorimeter test conducted at laboratory LMDC [18] (Figure 5) and adiabatic test conducted at laboratory CEBTP (Figure 6). The other parameters of the thermal model were taken directly from experimental results on the concrete (thermal conductivity and capacity, concrete density) and were assumed to be constant according to hydration development (Table 2).

As the material hardens, the instantaneous characteristics of concrete (strengths, Young’s modulus) have to be studied at several ages. In our approach, we consider variation laws expressed according to the hydration degree given by the multiphasic hydration model. The evolution of the characteristics used in the mechanical model is presented in Figure 7.

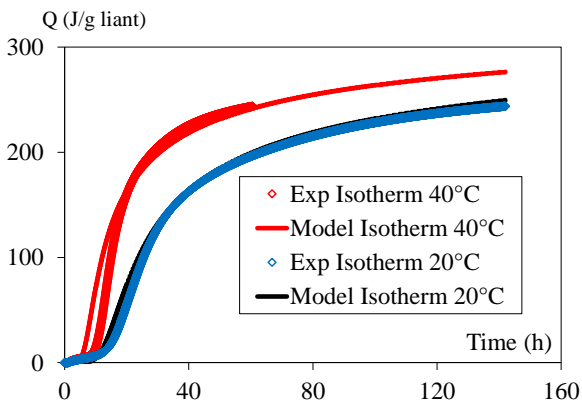


Figure 5: Calibration of heat of hydration of pure Portland cement (Isothermal calorimeter test at 20°C and 40°C) [18]

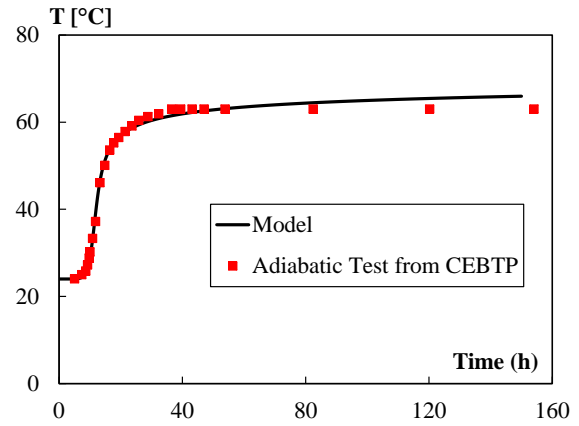
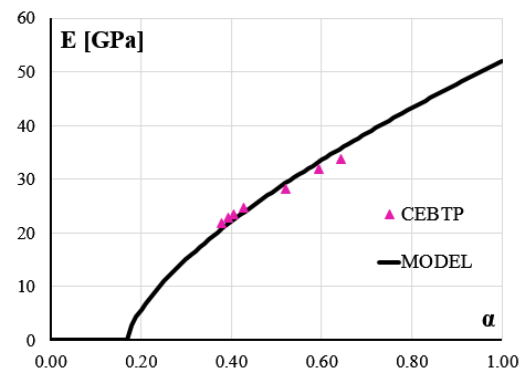


Figure 6: Prediction of temperature evolution of concrete in adiabatic condition (Adiabatic calorimeter test by CEBTP)

Table 2: Thermal parameters of concrete [12]

Thermal parameters	Quantities
Thermal conductivity (W/m. ⁰ C)	1.965
$\lambda[W/m.^{\circ}C]$	
Concrete density	2370
$(kg/m^3)\rho[kg/m^3]$	
Thermal capacity (J/kg. ⁰ C)	880
$C[J/kg.^{\circ}C]$	



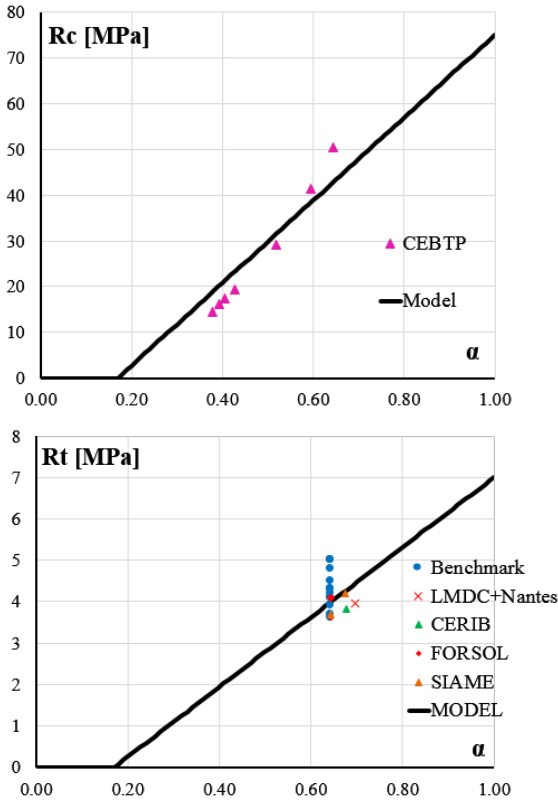


Figure 7: Evolution of instantaneous characteristics according to hydration development (experimental results obtained from different laboratories in MACENA project)

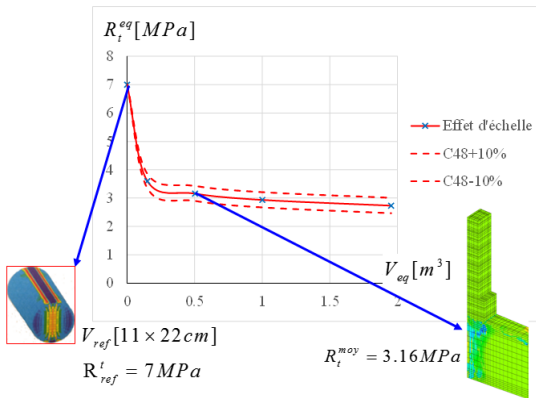


Figure 8: Evolution of tensile strength due to scale effect

4.3 Mesh and boundary condition

The studied structure was modelled using a 3D mesh with 27 840 cubic elements (Table 3). After several tests on the effect of mechanical boundary conditions, the soil under the

structure is also modelled and assumed to perform with elastic behavior (Figure 9).

Note that this work was granted access to the HPC resources of CALMIP supercomputing center under the allocation 2016-p16002 (<https://www.calmip.univ-toulouse.fr/>).

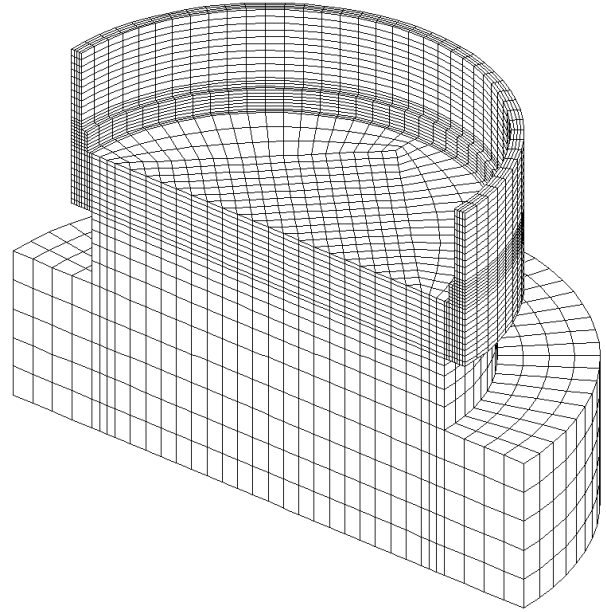


Figure 9: 3D mesh of the lower part of whole structure VerCoRs with soil (only a half of the structure is presented here)

Table 3: Number of meshed elements

Element	Number of 3D elements
Soil	4800
Pedestal	3200
Basement	12800
Gusset	3840
Internal wall-level 2	1600
Internal wall-level 3	1600

4.4 Thermal results

The calculation in this section is performed using the hydration model that is implemented in the finite element code Cast3M. Note that in this work, the continuous lines in the figures

are derived from modellings; the points correspond to experimental results.

Considering the equivalent and free convective coefficients for the period of formwork and after formwork removal, the external temperature variation plus the heating condition at gusset, the thermal results of modelling are in good agreement with the experimental measurements (Figure 10). Seeing these results, we note that it is important to carefully take all the boundary conditions and concrete characteristics into account.

As the model can reproduce well the evolution of temperature, its multiphysics characteristic also provides the evolution of porosity ϕ , water content W and hydration degree α , which will be used in the mechanical model to predict the cracking risk.

Moreover, the Figure 11 highlights the effect of using the concreting sequence method and how the mesh is exploited during the construction sequence. The first scheme shows the temperature field at 42h after casting gusset, the second one corresponds to temperature field at 20h after casting the second level of the internal wall, and the last one corresponds to temperature field at 22h after casting the third level of the internal wall.

If we take the first scheme as an example, we see that at 42h after casting gusset, the internal wall above the gusset has not yet been constructed, so the model activates only for gusset and basement but it has not activated yet for the above internal wall.

It can be seen clearly through the values of hydration and other parameters. The hydration of above internal wall has not yet developed, so the water content and porosity take its initial values and the temperature takes the value of imposed air temperature.

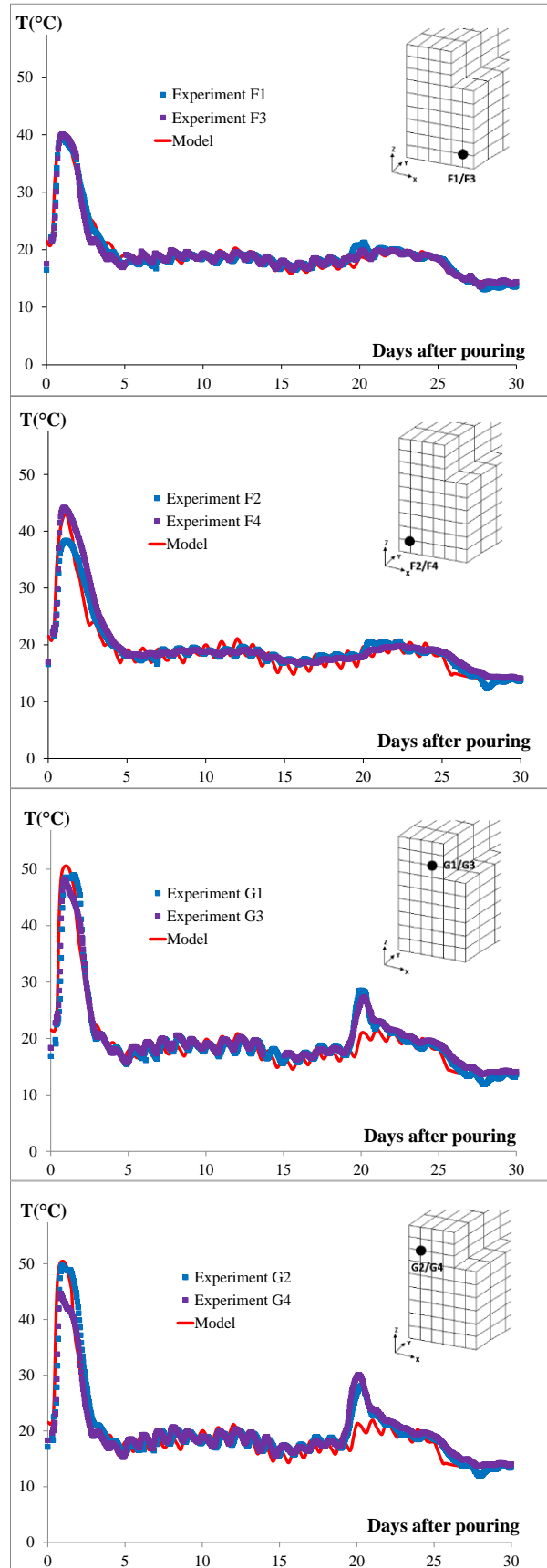


Figure 10: Numerical and experimental results for thermal evolution of gusset

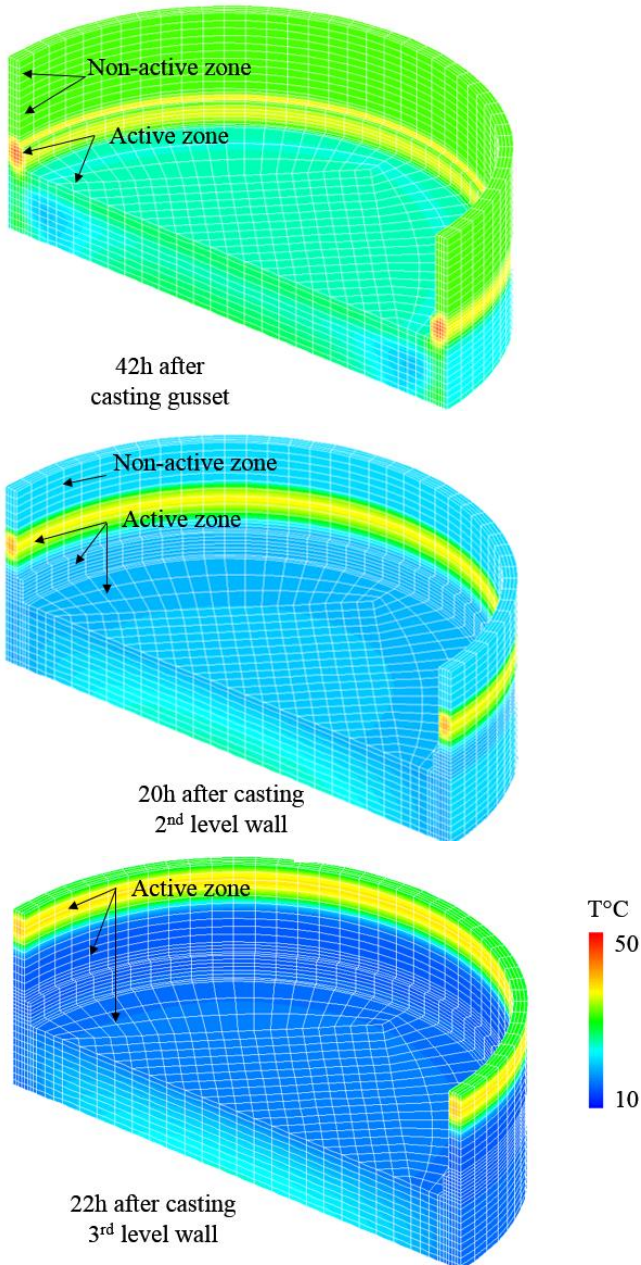


Figure 11: Temperature fields at different instance of construction sequence

4.5 Mechanical results

The schema in Figure 12 shows the maximal volume for the calculation of scale effect and the ratio of distributed reinforcements in three directions (the representation is made only of half of the structure but the entire structure is modelled).

Concerning mechanical boundary conditions of this second study, only the vertical displacement and rotation of the lower surface of the soil are blocked.

The thermal calculation last about 5 h and the mechanical calculation for the second study spend about 5 days on HPC resources of CALMIP supercomputing center (18 paralyzed processors at 2.4 GHz). The numerical results obtained from the THCM modelling were successfully compared with experimental results in terms of concrete strains (Figure 13).

The crack patterns obtained after casting gusset is also globally well reproduced (Figure 14). In this figure, the crack is more open in the basement. Concerning the crack width at gusset, the width is respected (less than 100 μm from model and experiment) but the order of magnitude is slightly overestimated (about 2000 μm for numerical results and between 750 and 1500 μm along the circumferential line observed experimentally).

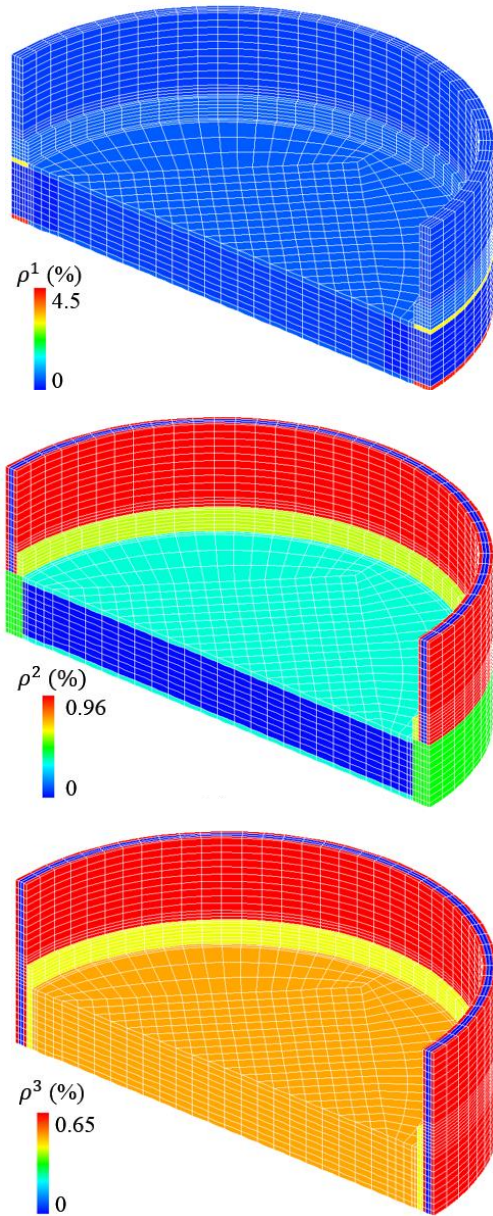


Figure 12: Repartition of distributed reinforcement ratio in radial, tangential, vertical direction respectively for a half of modelled structure

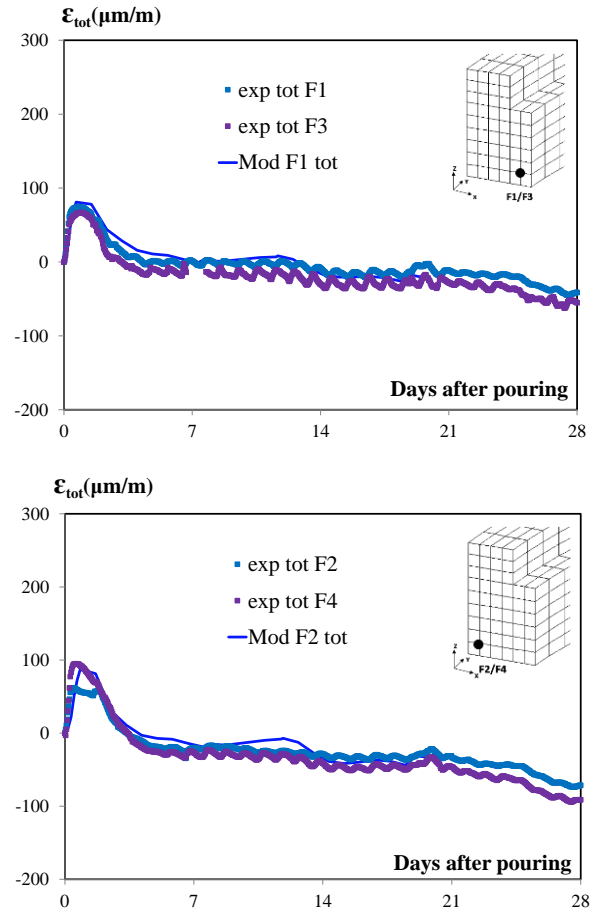


Figure 13: Comparison of measured (points) and numerical (blue curve) deformations at inner and outer face points

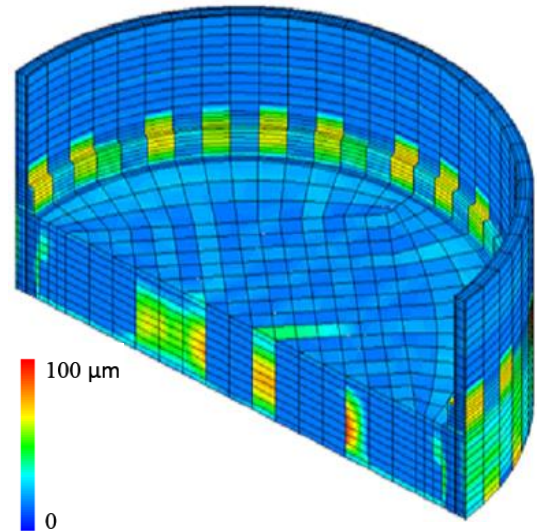


Figure 14: Numerical crack patterns for a half of modelled structure

5 CONCLUSIONS

This paper presents a numerical strategy that is adapted for “industrial” massive structures which are usually constructed by reinforced concrete and cast in successive layers. First, the strategy for concreting sequence modelling based on multiphasic hydration model is practical for an application to massive structures like VeRCoRs. The interest modelling the massive structure using this new method allows considering realistically the particularities of large structures, such as the sequential casting of concrete at a different date by avoiding to re-mesh the structure at each stage of casting. These considerations lead to obtaining a good prediction of the temperature evolution of VeRCoRs.

Furthermore, with good prediction of the temperature evolution and the consideration of reinforcement, the prediction of early-age cracking was globally good. Thus, this application highlighted the interest of modelling the distributed reinforcement without explicit meshing of reinforcements. It allowed to consider the structural effect of reinforcements on the global behavior of massive structure.

Finally, this study shows the importance of consideration of the probabilistic scale effect due to the material heterogeneity for forecasting the early-age cracking of massive structure. Short-term cracking in the lower parts of the containment (basement and gusset) due to temperature changes within the restrained structure at an early age is observed and modelled. This early age cracking has been identified at later ages as an important part of the causes of leakage of the structure and is thus of importance in the control of confinement.

ACKNOWLEDGEMENTS

We are grateful to EDF for construction of VeRCoRs and results reported here. The French National Research Agency (ANR) is acknowledged for their financial support to the project MACENA. We also thank to CEA for providing the finite element code Cast3M.

REFERENCES

- [1] L. Buffo-Lacarrière, A. Sellier, G. Escadeillas, and A. Turatsinze, “Multiphasic finite element modeling of concrete hydration,” *Cem. Concr. Res.*, vol. 37, no. 2, pp. 131–138, 2007.
- [2] L. Buffo-Lacarrière, A. Sellier, and B. Kolani, “Application of thermo-hydro-chemo-mechanical model for early age behaviour of concrete to experimental massive reinforced structures with strain-restraining system,” *Eur. J. Environ. Civ. Eng.*, vol. 18, no. 7, pp. 814–827, 2014.
- [3] A. Sellier, S. Multon, L. Buffo-Lacarrière, T. Vidal, X. Bourbon, and G. Camps, “Concrete creep modelling for structural applications: non-linearity, multi-axiality, hydration, temperature and drying effects,” *Cem. Concr. Res.*, vol. 79, pp. 301–315, 2016.
- [4] M. Azenha, C. Sousa, R. Faria, and A. Neves, “Thermo-hygro-mechanical modelling of self-induced stresses during the service life of RC structures,” *Eng. Struct.*, vol. 33, no. 12, pp. 3442–3453, 2011.
- [5] R. Lackner and H. A. Mang, “Chemoplastic material model for the simulation of early-age cracking: From the constitutive law to numerical analyses of massive concrete structures,” *Cem. Concr. Compos.* vol. 26, no. 5, pp. 551–562, 2004.
- [6] G. D. Schutter, “Fundamental study of early age concrete behaviour as a basis for durable concrete structures,” *Mater. Struct.*, vol. 35, no. 1, pp. 15–21, 2002.
- [7] F. Benboudjema and J. M. Torrenti, “Early-age behaviour of concrete nuclear containments,” *Nucl. Eng. Des.*, vol. 238, no. 10, pp. 2495–2506, 2008.
- [8] L. Buffo-Lacarrière, A. Sellier, A. Turatsinze, and G. Escadeillas, “Finite element modelling of hardening concrete: application to the prediction of early age cracking for massive reinforced

- structures,” *Mater. Struct.*, vol. 44, no. 10, pp. 1821–1835, 2011.
- [9] R. Faria, M. Azenha, and J. A. Figueiras, “Modelling of concrete at early ages: Application to an externally restrained slab,” *Cem. Concr. Compos.*, vol. 28, no. 6, pp. 572–585, 2006.
- [10] M. Azenha, R. Faria, and D. Ferreira, “Identification of early-age concrete temperatures and strains: Monitoring and numerical simulation,” *Cem. Concr. Compos.*, vol. 31, no. 6, pp. 369–378, 2009.
- [11] CEOS.fr, “French national research project for the design and assessment of special concrete structure with respect to cracking and shrinkage,” 2009. [Online]. Available: <http://www.ceosfr.irex.asso.fr/>.
- [12] EDF, “VeRCoRS Project: an experimental mock-up of a reactor containment-building,” 2014. [Online]. Available: <https://fr.xing-events.com/EDF-vercors-project.html>. [Accessed: 28-Jan-2016].
- [13] B. Kolani, L. Buffo-Lacarrière, A. Sellier, G. Escadeillas, L. Boutillon, and L. Linger, “Hydration of slag-blended cements,” *Cem. Concr. Compos.*, vol. 34, no. 9, pp. 1009–1018, Oct. 2012.
- [14] A. Sellier, G. Casaux-Ginestet, L. Buffo-Lacarrière, and X. Bourbon, “Orthotropic damage coupled with localized crack reclosure processing. Part I: Constitutive laws,” *Eng. Fract. Mech.*, vol. 97, pp. 148–167, Jan. 2013.
- [15] S. Ghavamian and A. Delaplace, “Modèles de fissuration de béton, Projet MECA,” *Rev. Fr. Génie Civ.*, vol. 7, no. 5, p. 172, 2003.
- [16] CEOS.fr, “Benchmark CEOS.fr : Fissuration sous chargement statique monotone, document de lancement du benchmark.” 2009.
- [17] B. Richard, F. Ragueneau, C. Cremona, and L. Adelaide, “Isotropic continuum damage mechanics for concrete under cyclic loading: Stiffness recovery, inelastic strains and frictional sliding,” *Eng. Fract. Mech.*, vol. 77, no. 8, pp. 1203–1223, 2010.
- [18] P. Chhun, “Modélisation du comportement thermo-hydro-chemo-mécanique des enceintes de confinement nucléaire en béton armé-précontraint,” phd, Université Toulouse III - Paul Sabatier, 2017.
- [19] A. Sellier and A. Millard, “Weakest link and localisation WL 2: a method to conciliate probabilistic and energetic scale effects in numerical models,” *Eur. J. Environ. Civ. Eng.*, vol. 18, pp. 1177–1191, 2014.